Am J Transl Res 2022;14(1):68-85
www.ajtr.org /ISSN:1943-8141/AJTR0124034

Original Article

The molecular mechanism of kinesin family member 2A (KIF2A) underlying non-small cell lung cancer: the effect of its knockdown on malignant behaviors, stemness, chemosensitivity, and potential regulated signaling pathways

Jiayan Chen[1,2], Junmiao Wen[1,2], Di Liu[1,2], Xinyan Xu[1,2], Min Fan[1,2], Zhen Zhang[1,2]

[1]Department of Radiation Oncology, Fudan University Shanghai Cancer Center, Shanghai, China; [2]Department of Oncology, Shanghai Medical College, Fudan University, Shanghai, China

Received October 13, 2020; Accepted January 26, 2021; Epub January 15, 2022; Published January 30, 2022

Abstract: Kinesin family member 2A (KIF2A) represents an oncogene in several cancers, however, its involvement in non-small cell lung cancer (NSCLC) is limitedly investigated. Therefore, the present study aimed to explore potential molecular mechanism of KIF2A knockdown in repressing NSCLC malignant behaviors. The effect of KIF2A knockdown on cell proliferation, apoptosis, invasion, epithelial-mesenchymal transition (EMT) markers, stemness, chemosensitivity was detected after transfecting KIF2A short hairpin RNA (ShRNA) plasmids into A549 and NCI-H1975 cells. Moreover, KIF2A knockdown mediated signaling pathways were analyzed by RNA sequencing (RNA-seq), and then validated by western blot assay. Both KIF2A mRNA and protein expressions were increased in A549, NCI-H650, NCI-H358, NCI-H2106, NCI-H1299, NCI-H1650 and NCI-H1975 cells compared with BEAS-2B cells. KIF2A knockdown inhibited proliferation, invasion, EMT, stemness, but enhanced chemosensitivity to cisplatin and paclitaxel in both A549 and NCI-H1975 cells. Meanwhile, it only promoted apoptosis in NCI-H1975 cells but not in A549 cells. Moreover, after KIF2A knocking down, RNA-seq data indicated that 356 accordant differentially expressed genes (DEGs) in both A549 and NCI-H1975 cells, and these DEGs were enriched in PI3K-Akt, Wnt and Notch signaling pathways. Further western blot disclosed that KIF2A knockdown indeed inactivated PI3K-Akt, Wnt and Notch signaling pathways in both A549 and NCI-H1975 cells. In conclusion, KIF2A knockdown suppresses NSCLC cell malignant behaviors, EMT and stemness, but enhances chemosensitivity via inactivating PI3K-Akt, Wnt, and Notch signaling pathways, which proposes it as a potential therapeutic target for NSCLC treatment.

Keywords: Kinesin family member 2A, non-small cell lung cancer, chemosensitivity, malignant behaviors, RNA-sequencing

Introduction

Lung cancer, the dominant cause of cancer-related mortality globally, comprises multiple histological and molecular subtypes, among which non-small cell lung cancer (NSCLC) is the most common diagnostic terms for lung cancer constituting approximately 80% newly diagnostic cases [1]. Only a small portion of NSCLC patients who are diagnosed at an early stage are available for curable surgical resection, and as for the majority of patients with advanced or metastatic status of NSCLC, curable surgery is inappropriate, and they normally suffer from undesirable 5-year survival rate [2-5]. Hence, improved understanding of the biology of NSCLC is of great importance, which might help to develop novel biomarker-targeted therapies, and further contribute to promotion of survival profiles as well as follow-up surveillance in NSCLC management.

Kinesin family member 2A (KIF2A) is one of the microtubule-depolymerizing kinesins belonging to kinesin 13 family, stimulating organization of microtubule cytoskeleton, and being implicated in microtubule-dynamics regulation [6]. Previous data demonstrates that KIF2A presents

with diverse functions during various aspect of biological and physiological processes, such as cellular division, chromosome localization, cell cycle alteration, cell differentiation, and etc. [6-9]. Increasing evidence has reported the involvement of KIF2A in the carcinogenesis of several cancers, via promoting cancer aggressive features and serving as an oncogenic mediator [7, 10-12]. For example, KIF2A is upregulated in gastric cancer cells (vs. normal gastric mucosa epithelial cells), and its silencing suppresses cell proliferation and presents inhibition on gastric tumor cell invasion via negatively affecting membrane type 1-matrix metalloproteinase [13]. In addition, KIF2A is involved in the process of facilitating the temozolomide resistance via PI3K/Akt signaling pathway, and there is evidence reporting that targeting KIF2A promotes the sensitivity of glioma cells to anti-microtubule chemotherapies [14, 15]. As for the role of KIF2A in NSCLC, only one study reports that KIF2A is clinically correlated with advanced tumor features and could serve as a biomarker for worse prognosis, however limited cellular experiments have reported the molecular mechanism of KIF2A in NSCLC, which is essential to be explored [12].

Hence, in the present study, we knocked down KIF2A in NSCLC via short hairpin RNA (ShRNA) in order to investigate the effect of KIF2A knockdown on NSCLC cell proliferation, apoptosis, invasion, epithelial-mesenchymal transition (EMT), stemness, chemosensitivity to cisplatin/paclitaxel, and subsequently conducted microarray assay, bioinformatic analysis and western blot to examine the potential signaling pathways regulated by KIF2A knockdown in NSCLC.

Methods

Cell culture

The A549 cells were grown in F-12K medium with 10% fetal bovine serum (FBS). And the culture medium for BEAS-2B, NCI-H650, NCI-H358, NCI-H1299, NCI-H1650 and NCI-H1975 cells was RPMI-1640 medium with 10% FBS. Then NCI-H1206 cells were cultured with DMEM/F12 medium supplemented with 10% FBS. All the cells and culture medium were purchased from the American Type Culture Collection (ATCC, USA) and Sigma-Aldrich (Sigma-Aldrich, USA), respectively. An atmosphere with 5% CO_2 was provided for the cell culture.

Plasmids construction and transfection

KIF2A ShRNA plasmids or negative control (NC) shRNA plasmid was generated by inserting hairpin or NC oligonucleotides into pGPH1 vector, which was obtained from Shanghai GenePharma Co., Ltd (Genepharma, China). When the A549 and NCI-H1975 reached 50-60% confluency, the HlilyMax (Dojindo, Japan) was applied for transfecting the KIF2A shRNA plasmids and NC shRNA plasmid into cells.

Cell proliferation and apoptosis assessment

After transfection, the cell counting kit-8 (Sigma, USA) reagent was added and incubated with cells for 2 hours (h) at 0 h, 24 h, 48 h and 72 h. Then the measurement of optical density (O D) value at 450 nm was performed to evaluate cell proliferation. Cell apoptosis was detected by Annexin V-FITC Apoptosis Detection Kit (eBioscience, USA) at 48 h after transfection with the kit's protocol was followed by.

Transwell invasion assay

At 24 h post the transfection, the cells were collected and mixed with serum-free culture medium and seeded onto the Matrigel Basement Membrane Matrix (BD, USA) coated chamber, which was then incubated in normal culture medium for 24 h. Subsequently, after wiping out the non-invasion cells, the cells attaching to the chamber were fixed with paraformaldehyde, stained with crystal violet and counted under a microscope.

Sphere formation and extreme limiting dilution analysis (ELDA)

At 24 h after transfection, the cells were collected and cultured in 24-well ultra-low attachment plates (Corning, USA) in serum-free DMEM/F12 medium (Sigma, USA) containing 5 μg/ml insulin (Sigma, USA), 10 ng/ml basic fibroblast growth factor (BD, USA), and 20 ng/ml recombinant human epidermal growth factor (BD, USA) for 7 days. The number of spheres with diagram >50 μm was counted. In terms of ELDA, different number (10, 100, 1000) of cells were plated in 24-well ultra-low attachment

plates (Corning, USA) for 24 well with medium mentioned above. After 7 days, the wells with at least 1 sphere (>50 μm) were counted and calculated with ELDA (http://bioinf.wehi.edu.au/software/elda/).

Flowcytometry

At 24 h after transfection, the CD133 positive ($CD133^+$) cell proportion was evaluated with flow cytometry. After collection, the cells were incubated with CD133 Mouse mAb (Alexa Fluor® 488 Conjugate) (CST, USA) in the dark for 1 h. Then the cells were acquired with a FACScan flow cytometer (BD, USA) and data were analyzed by Flowjo 10.0 (BD, USA).

Chemosensitivity assessment

At 24 h after transfection, cells were incubated with different concentrations of cisplatin (Sigma, USA) or paclitaxel (Sigma, USA) for 24 h. The concentrations of cisplatin (Sigma, USA) incubated with A549 and H1975 cells were 0, 1, 2, 4, 8, 16 μM and 0, 5, 10, 20, 40 and 80 μM, respectively. And the concentrations of paclitaxel (Sigma, USA) incubated with A549 and H1975 cells were 0, 5, 10, 20, 40, 80 nM. After the incubation, the CCK-8 (Sigma, USA) was used for cell viability assessment.

RNA sequencing (RNA-seq) and bioinformatics analysis

At 24 h after transfection, the A549 and NCI-H1975 cells transfected with Sh-NC and Sh-KIF2A plasmids were collected. Afterward, the TRIzol™ Reagent (Invitrogen, USA) was used to extract the total RNA of cells, and Agilent 2100 Bioanalyzer (Agilent, USA) was used to evaluate the concentration, purity, and integrity of the total RNA. At last, the sequencing library was constructed and sequenced according to the methods described in a previous study [16]. R packages (Version 3.3.3) were applied to complete RNA-seq data analysis and graph plotting. The raw data of each gene was calculated by feature count; the gene expression normalization and differentially expression analysis were performed with DESeq2. In addition, Factoextra package was applied to construct the principal component analysis (PCA) plots of mRNA profiles, and the pheatmap package was used to plot the heatmap of mRNA profiles. The mRNAs with fold change (FC)≥2.0 and adjusted *P* value (BH multiple test correction)<0.05 were defined as differentially expressed genes (DEGs) and presented with Volcano plots. The cross analysis was performed using VennDiagram package. KEGG (http://www.genome.jp/kegg) pathway enrichment analysis was performed using the DAVID website (https://david.ncifcrf.gov/) for the DEGs [17].

Reverse transcription quantitative polymerase chain reaction (RT-qPCR)

Total RNA was extracted using RNeasy Protect Mini Kit (Qiagen, Germany), and then the reverse transcription of total RNA to cDNA was performed using ReverTra Ace® qPCR RT Master Mix (Toyobo, Japan). Following which, qPCR was performed by SYBR® Green Realtime PCR Master Mix (Toyobo, Japan). The primers were as follow: KIF2A, forward 5' GCCGAATACATCAAGCAAT 3', reverse 5' CTCTCCAGGTCAATCTCTT 3'; GAPDH, forward 5' GACCACAGTCCATGCCATCAC 3'; reverse 5' ACGCCTGCTTCACCACCTT 3'.

Western blot

After the extraction of total protein using RIPA Lysis and Extraction Buffer (Thermo Fisher, USA), the protein quantitation was determined by Pierce™ BCA Protein Assay Kit (Thermo Fisher, USA). Then, the protein sample was separated by NuPAGE Bis-Tris Gels 4%-12% (Thermo Fisher, USA), and was further transferred onto the polyvinylidene fluoride membrane (Millipore, Germany). Last, the protein bands were visualized using Pierce™ ECL Plus Western Blotting Substrate (Thermo Fisher, USA). The antibodies applied in western blot were listed in **Table 1**.

Statistical analysis

All data was shown as mean and standard deviation (SD). GraphPad Prism 7.02 (GraphPad Software Inc., USA) was used for performing data analysis and graph plotting. One-way analysis of variance (ANOVA) followed by Dunnett's multiple comparisons test or Tukey's multiple comparisons test was performed for determining the multiple comparisons. $P<0.05$ was considered to be statistically significant. No significant was marked as NS. $P<0.05$, 0.01, and 0.001 were presented as *, ** and ***.

Table 1. Antibodies used in western blot

Antibody	Company	Dilution
Primary Antibody		
Rabbit polyclonal to KIF2A	Abcam (UK)	1:5000
Rabbit monoclonal to E-Cadherin	Abcam (UK)	1:20000
Rabbit monoclonal to N-Cadherin	Abcam (UK)	1:10000
Rabbit monoclonal to PI3K	Abcam (UK)	1:1000
Rabbit polyclonal to AKT	Abcam (UK)	1:1000
Rabbit polyclonal to p-AKT	CST (USA)	1:1000
Rabbit monoclonal to Notch1	Abcam (UK)	1:2000
Rabbit polyclonal to Notch2	Abcam (UK)	1:400
Rabbit polyclonal to WNT3A	Abcam (UK)	1:1000
Rabbit monoclonal to β-catenin	Abcam (UK)	1:8000
Rabbit monoclonal to GAPDH	CST (USA)	1:1000
Secondary Antibody		
Goat Anti-Rabbit IgG H&L (HRP)	Abcam (UK)	1:20000

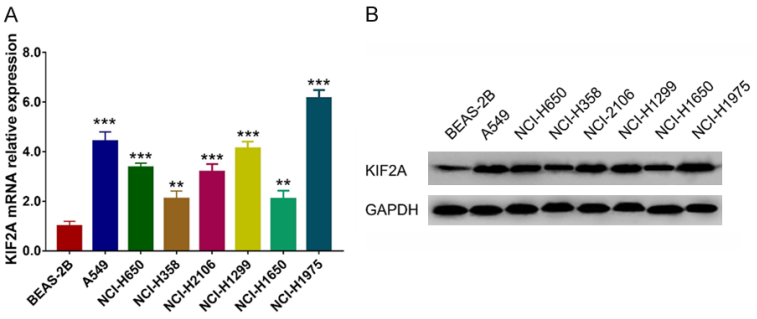

Figure 1. Comparison of KIF2A expression. Comparison of KIF2A mRNA (A) and protein (B) expressions between human NSCLC cell lines (A549, NCI-H650, NCI-H358, NCI-H2106, NCI-H1299, NCI-H1650, NCI-H1975 cell lines) and normal lung epithelial cell line (BEAS-2B cell line). KIF2A, kinesin family member 2A; NSCLC, non-small cell lung cancer.

Results

Comparison of KIF2A between human NSCLC cells and normal lung epithelial cells

Both KIF2A mRNA (**Figure 1A**) and protein (**Figure 1B**) expressions were increased in NSCLC cell lines (A549 (P<0.001), NCI-H650 (P<0.001), NCI-H358 (P<0.01), NCI-H2106 (P<0.001), NCI-H1299 (P<0.001), NCI-H1650 (P<0.01) and NCI-H1975 (P<0.001)) compared with BEAS-2B cells. Subsequently, A549 and NCI-H1975 cell lines were selected for further experimental studies.

KIF2A expression after transfection

To avoid off-target effect, three KIF2A ShRNA plasmids were transfected into A549 cells and NCI-H1975 cells, respectively. And the results disclosed that, in A549 cells, KIF2A mRNA (**Figure 2A**) and protein (**Figure 2B**) expressions were decreased in Sh-KIF2A1, Sh-KIF2A2 and Sh-KIF2A3 groups compared with Sh-NC group (all P<0.05). Meanwhile, in NCI-H1975 cells, after KIF2A knocking down, KIF2A mRNA (**Figure 2C**) and protein (**Figure 2D**) expressions were similar as those in A549 cells (all P<0.05). Given that Sh-KIF2A3 presented the best inhibitory effect on KIF2A expression, it was therefore chosen for the following experiments (referred as Sh-KIF2A afterword).

Effect of KIF2A knockdown on proliferation and apoptosis

In A549 cells, cell viability was decreased in Sh-KIF2A group compared with Sh-NC group at 72 h (P<0.05) after transfection (**Figure 3A**). Furthermore, cell apoptosis presented an increased trend in Sh-KIF2A group compared with Sh-NC group, but without statistical significance (P>0.05) (**Figure 3B**, **3C**). As for in NCI-H1975 cells, cell viability was reduced in Sh-KIF2A group compared with Sh-NC group at 48 h (P<0.05) and 72 h (P<0.01) after transfection (**Figure 3D**). Meanwhile, cell apoptosis was higher in Sh-KIF2A group compared with Sh-NC group (P<0.001) (**Figure 3E**, **3F**).

Effect of KIF2A knockdown on invasion and EMT

In A549 cells, invasive cell count was decreased in Sh-KIF2A group compared with Sh-NC group (P<0.05) (**Figure 4A**, **4B**). Moreover, E-cadherin protein expression was increased, while N-cadherin protein expression was reduced in Sh-KIF2A group compared with Sh-NC group (**Figure 4C**). Meanwhile, in NCI-H1975 cells, the effects of Sh-KIF2A on cell invasion (P<0.01) (**Figure 4D**, **4E**) and E-cadherin,

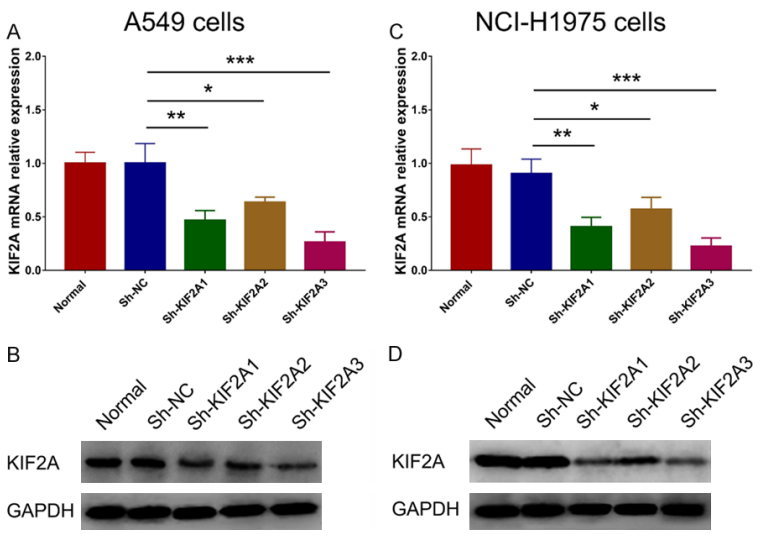

Figure 2. KIF2A expression of transfected NSCLC cells. After transfecting three KIF2A ShRNA plasmids into A549 (A, B) and NCI-H1975 (C, D) cells, comparisons of KIF2A mRNA and protein expressions between Sh-KIF2A1, Sh-KIF2A2, Sh-KIF2A3 groups and Sh-NC group, respectively. KIF2A, kinesin family member 2A; NSCLC, non-small cell lung cancer; Sh, short hairpin RNA; NC, negative control.

N-cadherin protein expressions (**Figure 4F**) were similar as in A549 cells.

Effect of KIF2A knockdown on stemness

In A549 cells, the sphere number per 1000 cells was reduced in Sh-KIF2A group compared with Sh-NC group (P<0.05) (**Figure 5A**). Besides, the estimated stem cell frequency was lower in Sh-KIF2A group compared with Sh-NC group by ELDA assay (1 per 363 cells vs. 1 per 156 cells) (P<0.01) (**Table 2**). Furthermore, $CD133^+$ cells proportion was decreased in Sh-KIF2A group compared with Sh-NC group (P< 0.05) (**Figure 5B**, **5C**). Furthermore, as for in NCI-H1975 cells, the effects of Sh-KIF2A on sphere formation ability (both P<0.01) (**Figure 5D**; **Table 2**) and $CD133^+$ cells proportion (P<0.01) (**Figure 5E**, **5F**) were similar as in A549 cells.

Effect of KIF2A knockdown on chemosensitivity to cisplatin and paclitaxel

In A549 cells, relative cell viability was reduced in 2 μM (P<0.05), 4 μM (P<0.05) and 8 μM (P< 0.05) cisplatin-treated Sh-KIF2A group compared with Sh-NC group (**Figure 6A**). Meanwhile, relative cell viability was deceased in 5 nM (P<0.05), 10 nM (P<0.05), 20 nM (P<0.05), 40 nM (P<0.05), 80 nM (P<0.05) paclitaxel-treated Sh-KIF2A group compared with Sh-NC group (**Figure 6B**). Regarding in NCI-H1975 cells, relative cell viability was decreased in 10 μM (P<0.05), 20 μM (P<0.05), 40 μM (P<0.05), 80 μM (P<0.05) cisplatin-treated Sh-KIF2A group compared with Sh-NC group (**Figure 6C**). Meanwhile, relative cell viability was reduced in 5 nM (P<0.05), 10 nM (P< 0.05), 20 nM (P<0.05) paclitaxel-treated Sh-KIF2A group compared with Sh-NC group (**Figure 6D**). These data indicated that Sh-KIF2A promoted chemosensitivity to cisplatin and paclitaxel in NSCLC cells.

mRNA expression profiles by KIF2A knockdown

RNA-seq assay was performed after the transfection of Sh-KIF2A plasmid into A549 and NCI-H1975 cells. In A549 cells, PCA plots displayed a clear segregation of mRNA expression profiles between Sh-KIF2A group and Sh-NC group (**Figure 7A**), and the heatmap analysis exhibited a relatively good consistency and tendency of mRNA expression profiles by KIF2A knockdown (**Figure 7B**). As for the results in NCI-H1975 cells, a clear segregation of mRNA profiles (**Figure 7C**), as well as a relatively good consistency and tendency of mRNA expression profiles (**Figure 7D**) between Sh-KIF2A group and Sh-NC group were shown.

Enrichment analysis for DEGs by KIF2A knockdown

In A549 cells, volcano plots exhibited that 792 DEGS were upregulated, and 585 DEGs were downregulated in Sh-KIF2A group compared with Sh-NC group (**Figure 8A**). Further KEGG enrichment analysis exhibited that DEGs by KIF2A knockdown were mainly enriched in Notch signaling pathway, Wnt signaling pathway, PI3K-Akt signaling pathway, and etc. (**Figure 8B**). As for in NCI-H1975 cells, 829 DEGs were upregulated, and 281 DEGs were downregulated in Sh-KIF2A group compared with Sh-NC group (**Figure 8C**). DEGs by KIF2A knockdown were mainly enriched in Wnt signaling pathway, Notch signaling pathway, VEGF signaling pathway, and etc. (**Figure 8D**).

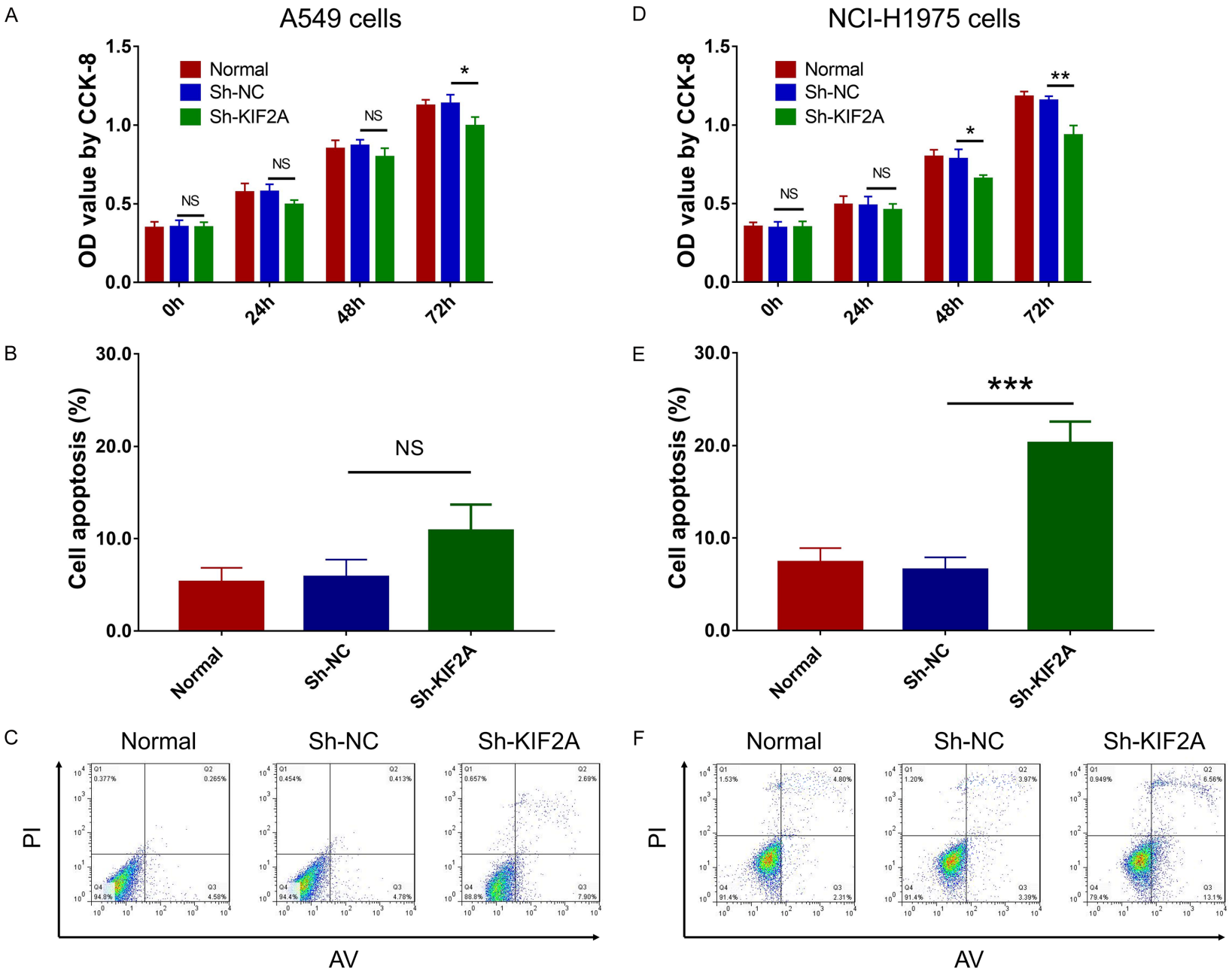
A
A549 cells
OD value by CCK-8
Normal
Sh-NC
Sh-KIF2A
NS
NS
NS
*
0h
24h
48h
72h
D
NCI-H1975 cells
OD value by CCK-8
NS
NS
*
**
B
Cell apoptosis (%)
NS
Normal
Sh-NC
Sh-KIF2A
E
Cell apoptosis (%)
***
C
Normal
Sh-NC
Sh-KIF2A
PI
AV
F

Figure 3. Comparison of cell proliferation and apoptosis. Comparison of cell proliferation (A), cell apoptosis (B, C) between Sh-KIF2A group and Sh-NC group in A549 cells. Comparison of cell proliferation (D), cell apoptosis (E, F) between Sh-KIF2A group and Sh-NC group in NCI-H1975 cells. KIF2A, kinesin family member 2A; Sh, short hairpin RNA; NC, negative control; OD, optical density; CCK-8, cell counting kit-8.

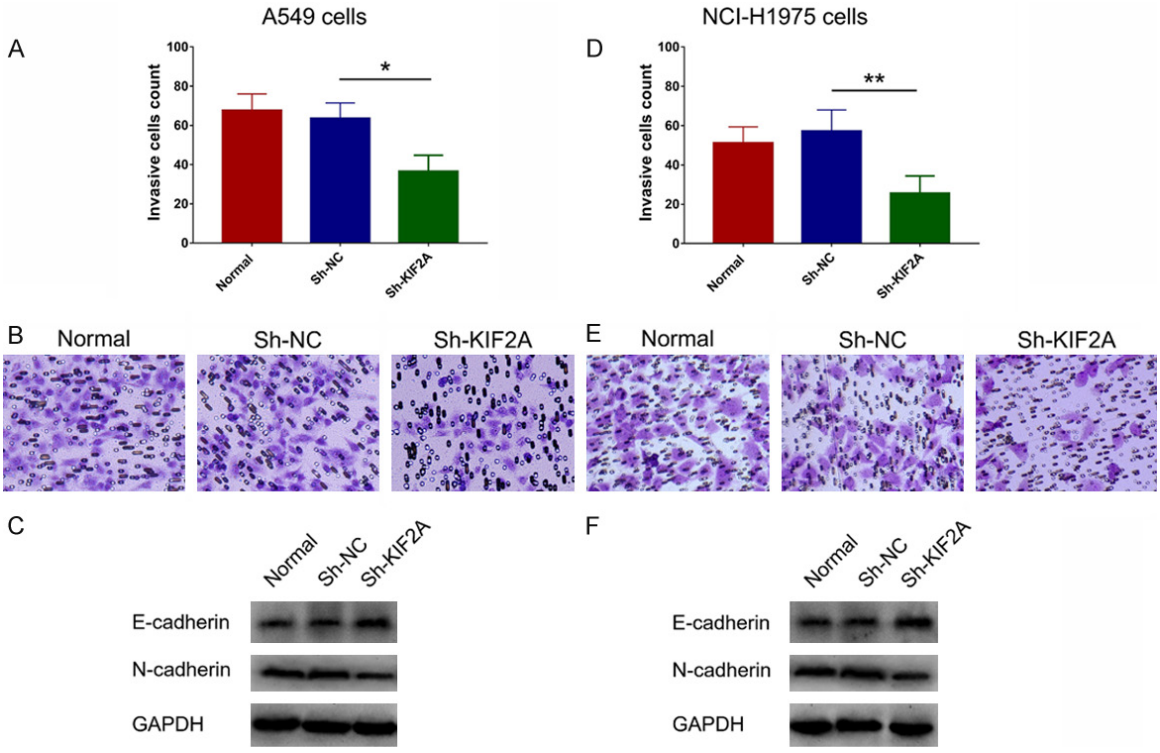

Figure 4. Comparison of cell invasion and EMT markers. Comparison of invasive cells count (A, B), expressions of EMT markers (C) between Sh-KIF2A group and Sh-NC group in A549 cells. Comparison of invasive cells count (D, E), expressions of EMT markers (F) between Sh-KIF2A group and Sh-NC group in NCI-H1975 cells. KIF2A, kinesin family member 2A; Sh, short hairpin RNA; NC, negative control.

Enrichment analysis for accordant DEGs by KIF2A knockdown

Cross analysis was performed to illustrate the overlapping patters of the accordant DEGs in Sh-KIF2A group vs. Sh-NC group of A549 cells and NCI-H1975 cells (**Figure 9A**). Totally, 292 accordant DEGs were upregulated in the Sh-KIF2A group (vs. Sh-NC group) in both two cell lines, and 64 accordant DEGs were downregulated in the Sh-KIF2A group (vs. Sh-NC group) in both two cell lines. The information of top 60 accordant DEGs by KIF2A knockdown in A549 and NCI-H1975 cells was shown in **Table 3**. Further KEGG enrichment analysis showed that these accordant DEGs were enriched in Notch signaling pathway, PI3K-Akt signaling pathway, Wnt signaling pathways and etc. (**Figure 9B**). In addition, the information about top 10 pathways with accordant DEGs from KEGG enrichment analysis was exhibited in **Table 4**.

Effect of KIF2A knockdown on PI3K-Akt, Notch and Wnt signaling pathways

According to the results from the KEGG enrichment analysis of the accordant DEGs, PI3K-Akt, Notch and Wnt signaling pathways, which closely associated with carcinogenic, chemosensitivity-related processes and stemness of NSCLC, were screened out. Therefore, the following western blot analysis was conducted to validate the effect of KIF2A knockdown on these three signaling pathways in NSCLC. In A549 cells, western blotting visualized that PI3K, p-AKT, Notch 1, Notch 2, WNT3A and β-catenin expressions were decreased in Sh-KIF2A group compared with Sh-NC group (**Figure 10A**). Moreover, in NCI-H1975 cells, they presented the same trends (**Figure 10B**).

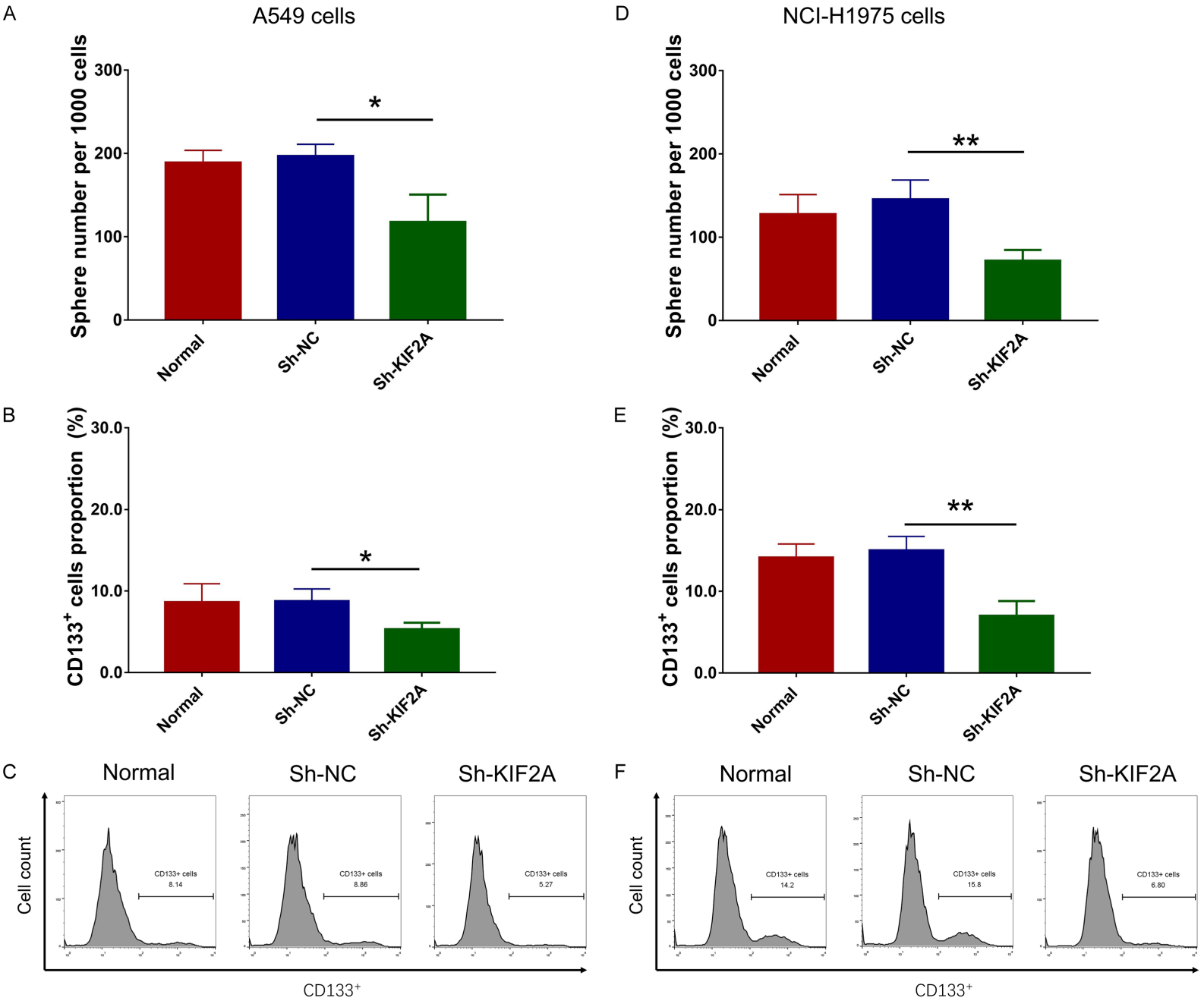
A
A549 cells
Sphere number per 1000 cells
300
200
100
0
*
Normal
Sh-NC
Sh-KIF2A
D
NCI-H1975 cells
Sphere number per 1000 cells
300
200
100
0
**
Normal
Sh-NC
Sh-KIF2A
B
CD133+ cells proportion (%)
30.0
20.0
10.0
0.0
*
Normal
Sh-NC
Sh-KIF2A
E
CD133+ cells proportion (%)
30.0
20.0
10.0
0.0
**
Normal
Sh-NC
Sh-KIF2A
C
Normal
Sh-NC
Sh-KIF2A
Cell count
CD133+ cells
8.14
CD133+ cells
8.86
CD133+ cells
5.27
CD133+
F
Normal
Sh-NC
Sh-KIF2A
Cell count
CD133+ cells
14.2
CD133+ cells
15.8
CD133+ cells
6.80
CD133+

Figure 5. Comparison of stemness. Comparison of sphere formation ability (A), and CD133$^+$ cells proportion (B, C) between Sh-KIF2A group and Sh-NC group in A549 cells. Comparison of sphere formation ability (D), and CD133$^+$ cells proportion (E, F) between Sh-KIF2A group and Sh-NC group in NCI-H1975 cells. KIF2A, kinesin family member 2A; Sh, short hairpin RNA; NC, negative control.

Table 2. ELDA data

Groups	Limiting dilution (wells)			1/stem cell frequency			*P* value
	1000	100	10	lower	estimate	upper	
A549 Cells							
Normal	22/24	12/24	8/24	322	192	114.5	
Sh-NC	23/24	11/24	8/24	263	156	92.7	0.00854
Sh-KIF2A	19/24	10/24	6/24	571	363	231.1	
NCI-H1975 Cells							
Normal	23/24	15/24	12/24	163	100.7	62.2	
Sh-NC	24/24	16/24	11/24	91	58.4	37.6	0.00051
Sh-KIF2A	22/24	13/24	8/24	305	181.5	108.0	

ELDA, Extreme Limiting Dilution Analysis.

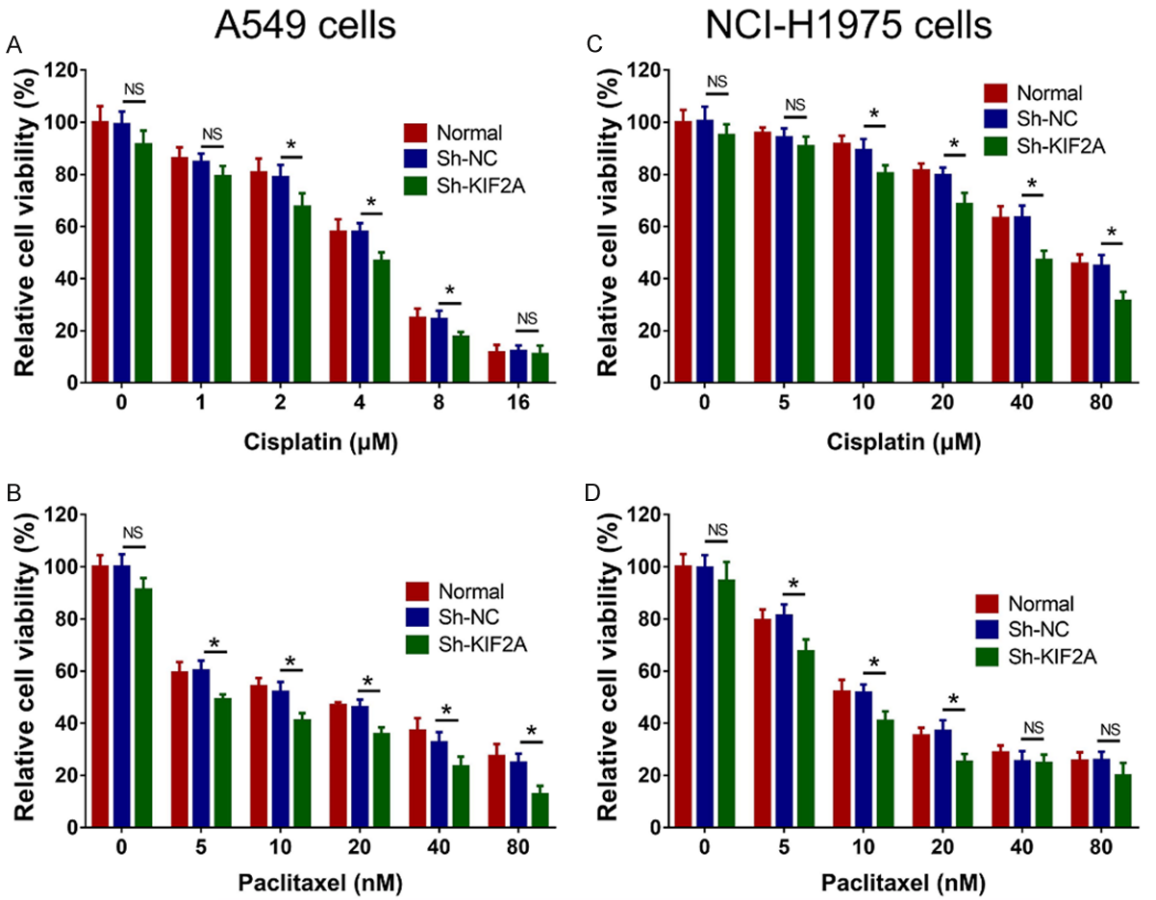

Figure 6. Comparison of chemosensitivity. Comparison of relative cell viability between Sh-KIF2A group and Sh-NC group treated with different concentration of cisplatin (A) and paclitaxel (B) in A549 cells. Comparison of relative cell viability between Sh-KIF2A group and Sh-NC group treated with different concentration of cisplatin (C) and paclitaxel (D) in NCI-H1975 cells. KIF2A, kinesin family member 2A; Sh, short hairpin RNA; NC, negative control.

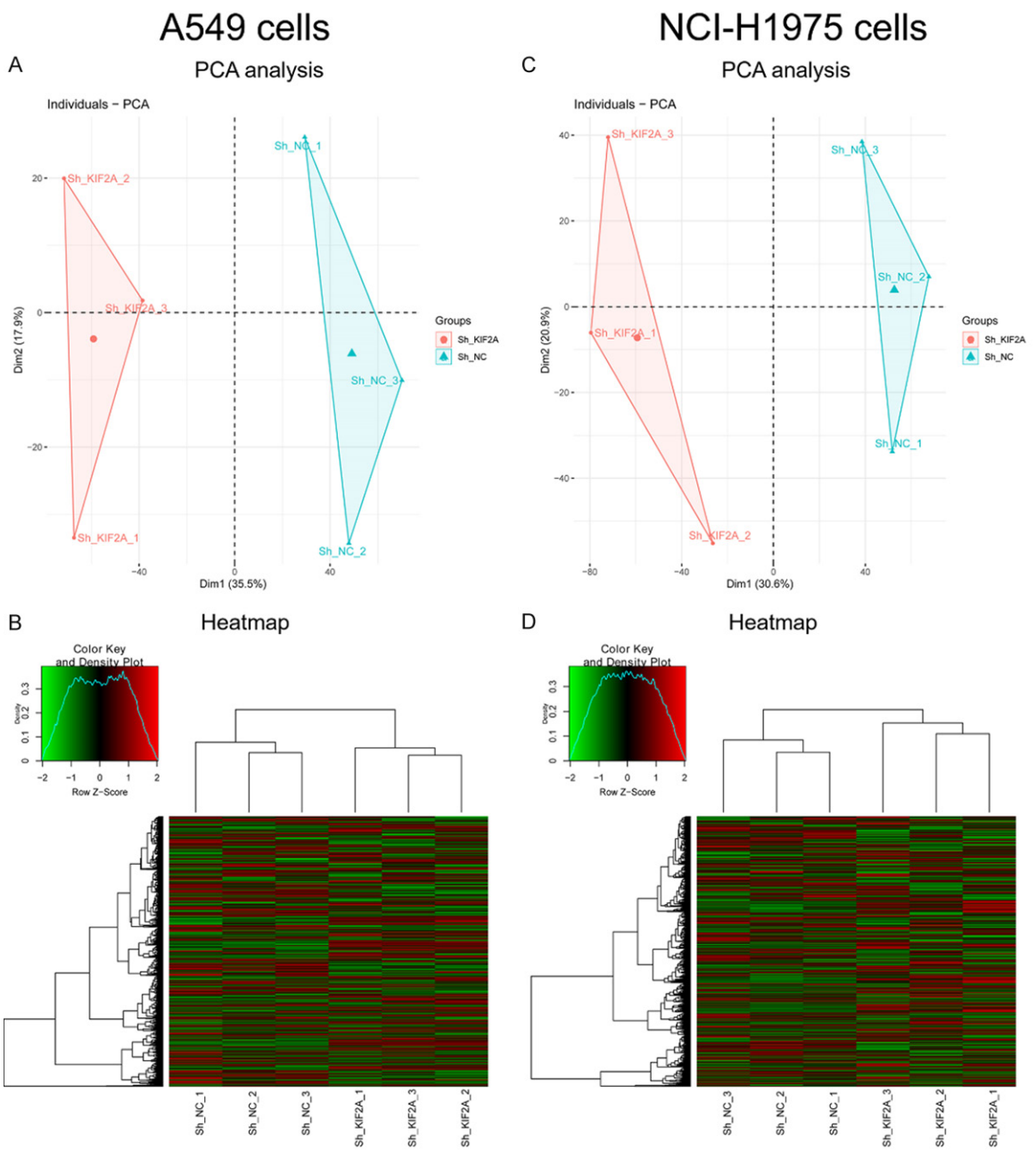

Figure 7. PCA plots and heatmap analysis. PCA plot (A) and heatmap analysis (B) for mRNA profiles by KIF2A knockdown in A549 cells. PCA plot (C) and heatmap analysis (D) for DEGs by KIF2A knockdown in NCI-H1975 cells. KIF2A, kinesin family member 2A; Sh, short hairpin RNA; NC, negative control; PCA, principal component analysis.

Discussion

In the present study, the summarized results included that (1) KIF2A was upregulated in NSCLC cells compared with normal lung epithelial cells. (2) KIF2A knockdown inhibited the malignant behaviors of NSCLC cells, such as cell proliferation, invasion, EMT progression, but promoted apoptosis. (3) KIF2A knockdown suppressed stemness, but enhanced chemosensitivity to cisplatin and paclitaxel in NSCLC cells. (4) KIF2A knockdown inactivated PI3K-Akt, Wnt and Notch signaling pathways in NSCLC derived from RNA-seq discovery, and these data were further validated by western blot assay.

KIF2A serves as a microtubule depolymerase implicated in microtubule-dependent biological process, such as cell mitosis, cell division, cell-

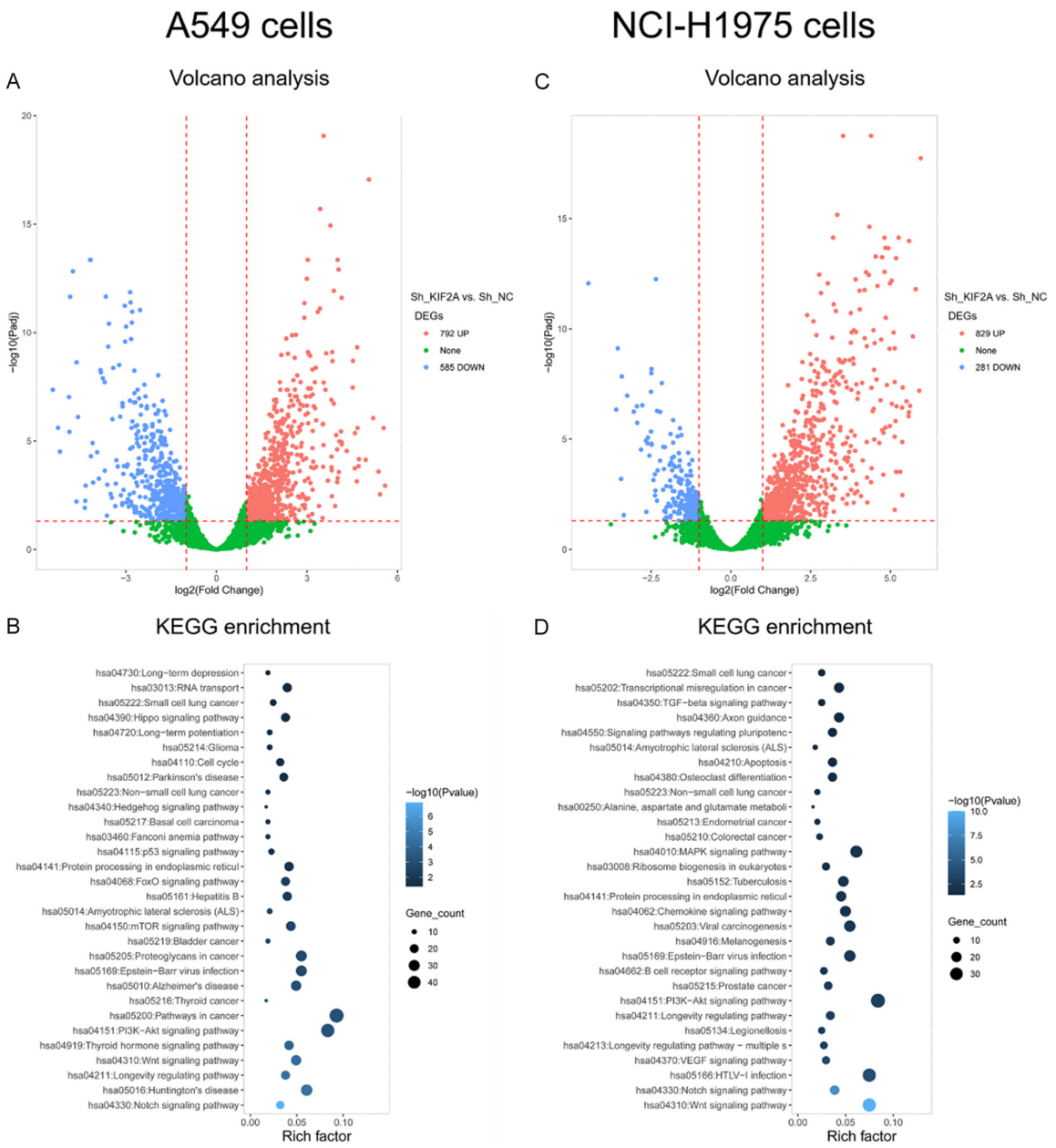

Figure 8. Volcano plot and KEGG enrichment analysis. Volcano plot (A), KEGG enrichment analysis (B) for DEGs by KIF2A knockdown in A549 cells. Volcano plot (C), KEGG enrichment analysis (D) for DEGs by KIF2A knockdown in NCI-H1975 cells. KIF2A, kinesin family member 2A; Sh, short hairpin RNA; NC, negative control; DEGs, differentially expression genes.

fate specification, and is involved in the pathological process of several genetic diseases [18-20]. For example, one previous study illustrates that aberrant KIF2A participates in the disorders of cell proliferation, differentiation, regulating neurological impairment and malformation of cortical development [19]. Recently, KIF2A has attracted increasing attention from researchers considering its oncogenic role in the carcinogenesis of several tumors, and findings from several functional studies illuminate that KIF2A promotes proliferation, migration, and invasion, while suppresses apoptosis of malignant cells via several means, initiating and promoting malignant development [7, 10-13, 18]. For instance, one prior study illustrates that silencing KIF2A promotes cell apoptosis, but inhibits invasion and migration via

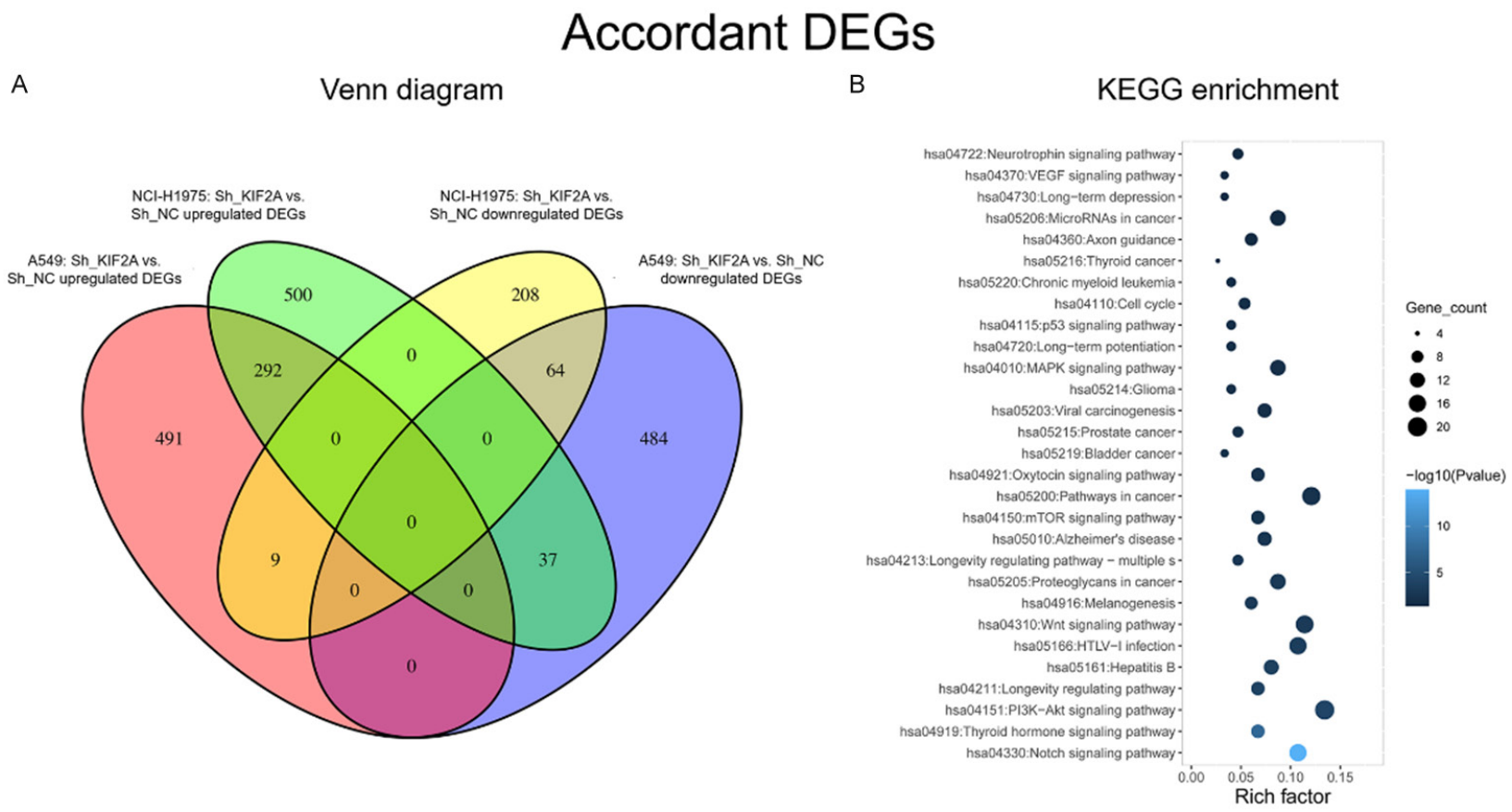

Figure 9. Venn diagram and KEGG enrichment analysis for accordant DEGs. Venn diagram analysis for the accordant DEGs by KIF2A knockdown in both A549 and NCI-H1975 cells (A). KEGG enrichment analysis for these accordant DEGs (B). KIF2A, kinesin family member 2A; Sh, short hairpin RNA; NC, negative control; DEGs, differentially expression genes.

Table 3. Top 60 accordant DEGs by RNA-seq

Gene ID	Symbol	A549: Sh_KIF2A vs. Sh_NC				NCI-H1975: Sh_KIF2A vs. Sh_NC				Mean ABS log_2FC
		log_2FC	*P* value	P_{adj} value	Trend	log_2FC	*P* value	P_{adj} value	Trend	
ENSG00000099974	DDTL	5.4163	0.000145293	0.002865059	UP	5.3779	0.000151894	0.003427768	UP	5.3971
ENSG00000137040	RANBP6	5.3673	7.73346E-06	0.000255102	UP	5.3067	9.03827E-06	0.000304573	UP	5.3370
ENSG00000102967	DHODH	5.1903	9.49346E-09	8.727E-07	UP	4.7509	5.99957E-08	3.88635E-06	UP	4.9706
ENSG00000105989	WNT2	5.5371	3.37062E-08	2.50831E-06	UP	4.2694	1.75181E-05	0.000548899	UP	4.9032
ENSG00000196456	ZNF775	4.5872	6.44277E-08	4.33051E-06	UP	5.0456	2.81574E-09	2.4964E-07	UP	4.8164
ENSG00000082213	C5orf22	3.9312	0.000711895	0.009913794	UP	5.1841	9.01345E-06	0.000304557	UP	4.5577
ENSG00000134259	NGF	3.1846	8.01053E-05	0.001756975	UP	5.3870	4.16943E-10	4.57248E-08	UP	4.2858
ENSG00000142156	COL6A1	4.9425	1.80849E-06	7.36473E-05	UP	3.6289	0.000473012	0.008460074	UP	4.2857
ENSG00000004776	HSPB6	3.3012	1.25E-08	1.11074E-06	UP	5.1372	3.73359E-12	7.65201E-10	UP	4.2192
ENSG00000124784	RIOK1	3.2280	5.17659E-06	0.000180272	UP	5.1029	5.97549E-13	1.46481E-10	UP	4.1655
ENSG00000146540	C7orf50	2.6161	0.004440116	0.03925766	UP	5.6166	3.59268E-09	3.07641E-07	UP	4.1164
ENSG00000007968	E2F2	3.3563	2.66366E-14	1.11004E-11	UP	4.8170	6.01169E-18	7.41704E-15	UP	4.0866
ENSG00000172845	SP3	2.5628	0.002486107	0.025665819	UP	5.5709	1.20586E-08	9.08172E-07	UP	4.0669
ENSG00000168172	HOOK3	4.6619	1.56203E-12	4.76305E-10	UP	3.4342	4.27142E-08	2.82546E-06	UP	4.0481
ENSG00000240682	ISY1	2.5887	0.001037501	0.01318174	UP	5.3663	4.46507E-09	3.72148E-07	UP	3.9775
ENSG00000269693	CTD-2192J16.20	2.1672	0.002834583	0.028237418	UP	5.7051	9.3324E-13	2.20139E-10	UP	3.9362
ENSG00000011523	CEP68	3.6338	3.19742E-12	9.08503E-10	UP	4.1922	4.32876E-15	1.74575E-12	UP	3.9130
ENSG00000006652	IFRD1	4.0002	3.03806E-05	0.000788004	UP	3.6632	0.000143802	0.003286871	UP	3.8317
ENSG00000102606	ARHGEF7	4.1456	4.58267E-15	2.49098E-12	UP	3.5168	1.95361E-11	3.34576E-09	UP	3.8312
ENSG00000204524	ZNF805	1.7050	0.000136439	0.002737977	UP	5.9535	8.86406E-22	1.84697E-18	UP	3.8292
ENSG00000141556	TBCD	2.5031	0.001190359	0.014633101	UP	5.1348	2.07599E-10	2.5697E-08	UP	3.8189
ENSG00000157734	SNX22	2.0298	0.000272014	0.004756247	UP	5.5874	9.98577E-18	1.04035E-14	UP	3.8086
ENSG00000117036	ETV3	4.1247	5.20123E-08	3.59258E-06	UP	3.4303	5.69215E-06	0.000207473	UP	3.7775
ENSG00000115687	PASK	2.1355	9.00445E-05	0.001934254	UP	5.2580	6.52595E-18	7.41704E-15	UP	3.6968
ENSG00000157193	LRP8	3.8092	9.29644E-10	1.27719E-07	UP	3.5137	3.35279E-07	1.70393E-05	UP	3.6614
ENSG00000125430	HS3ST3B1	2.2934	0.000900818	0.011755769	UP	4.9736	3.98316E-12	8.03186E-10	UP	3.6335
ENSG00000111266	DUSP16	2.5833	0.00240053	0.025022836	UP	4.6527	2.82011E-07	1.48139E-05	UP	3.6180
ENSG00000048540	LMO3	2.3644	2.32278E-06	9.13187E-05	UP	4.8550	1.08441E-13	3.15287E-11	UP	3.6097
ENSG00000136319	TTC5	2.2583	1.50013E-05	0.00043114	UP	4.8212	3.78283E-16	2.62739E-13	UP	3.5398
ENSG00000145002	FAM86B2	2.7987	3.48299E-07	1.80682E-05	UP	4.2626	2.88088E-12	6.10453E-10	UP	3.5306
ENSG00000144791	LIMD1	-4.3575	0.000933087	0.012088557	DN	-2.6595	2.13066E-07	1.17346E-05	DN	3.5085
ENSG00000159842	ABR	-2.7974	0.000642174	0.00915446	DN	-3.4392	2.05429E-05	0.00063571	DN	3.1183

ENSG00000156162	DPY19L4	-2.8113	3.30743E-08	2.47602E-06	DN	-3.4182	1.04999E-10	1.44252E-08	DN	3.1148
ENSG00000188549	C15orf52	-2.4813	9.09612E-06	0.000286447	DN	-3.5420	3.66528E-12	7.63721E-10	DN	3.0117
ENSG00000166783	KIAA0430	-4.1800	4.95293E-17	4.42632E-14	DN	-1.7800	0.000395466	0.007477927	DN	2.9800
ENSG00000088812	ATRN	-3.1854	8.07798E-09	7.53663E-07	DN	-2.5536	1.27679E-06	5.60083E-05	DN	2.8695
ENSG00000116157	GPX7	-3.7606	6.34035E-11	1.2785E-08	DN	-1.7797	0.001404402	0.019661625	DN	2.7702
ENSG00000182575	NXPH3	-2.3365	1.38363E-05	0.000401054	DN	-2.9354	2.62662E-08	1.81425E-06	DN	2.6359
ENSG00000107929	LARP4B	-2.7166	2.62454E-11	5.65725E-09	DN	-2.5037	7.05959E-10	7.11767E-08	DN	2.6101
ENSG00000103187	COTL1	-3.5823	1.42344E-12	4.44897E-10	DN	-1.6007	0.001674374	0.022703926	DN	2.5915
ENSG00000196923	PDLIM7	-2.8634	1.04886E-09	1.38029E-07	DN	-2.2177	2.2846E-06	9.42644E-05	DN	2.5406
ENSG00000213337	ANKRD39	-1.7791	0.00096033	0.012364625	DN	-3.2503	1.11507E-09	1.07235E-07	DN	2.5147
ENSG00000146072	TNFRSF21	-3.5566	1.02791E-13	3.89421E-11	DN	-1.4715	0.000925603	0.014233571	DN	2.5140
ENSG00000100625	SIX4	-1.9079	0.000134219	0.002710842	DN	-2.9433	3.83275E-09	3.23764E-07	DN	2.4256
ENSG00000116106	EPHA4	-2.8248	6.04975E-13	1.99037E-10	DN	-1.8450	1.66931E-06	7.14715E-05	DN	2.3349
ENSG00000138640	FAM13A	-2.1234	4.33475E-07	2.1852E-05	DN	-2.1167	4.53349E-07	2.22265E-05	DN	2.1201
ENSG00000140682	TGFB1I1	-2.0965	3.30011E-07	1.72628E-05	DN	-2.0684	4.73149E-07	2.30253E-05	DN	2.0825
ENSG00000020577	SAMD4A	-1.7833	1.07745E-09	1.40316E-07	DN	-2.3487	9.78423E-16	5.56011E-13	DN	2.0660
ENSG00000168067	MAP4K2	-2.5614	7.70292E-10	1.08204E-07	DN	-1.4362	0.000565257	0.009733946	DN	1.9988
ENSG00000130529	TRPM4	-2.6125	2.66236E-10	4.35124E-08	DN	-1.3819	0.000664616	0.011034574	DN	1.9972
ENSG00000233757	AC092835.2	-2.3739	2.37575E-08	1.90395E-06	DN	-1.5322	0.000305268	0.005991305	DN	1.9531
ENSG00000213614	HEXA	-2.0932	0.000193392	0.003597903	DN	-1.7291	0.000389752	0.007405281	DN	1.9112
ENSG00000106635	BCL7B	-1.4898	0.000187289	0.003521026	DN	-2.3140	6.53381E-09	5.23626E-07	DN	1.9019
ENSG00000196976	LAGE3	-1.8785	0.002701489	0.027303167	DN	-1.8874	0.002301138	0.029147753	DN	1.8830
ENSG00000125835	SNRPB	-2.0812	0.000334274	0.005524836	DN	-1.6326	0.004823318	0.049025306	DN	1.8569
ENSG00000119723	COQ6	-1.5515	0.000871572	0.011518389	DN	-2.0972	6.29183E-06	0.000226213	DN	1.8244
ENSG00000081041	CXCL2	-1.1379	0.002886038	0.028590529	DN	-2.4901	7.10528E-11	1.02104E-08	DN	1.8140
ENSG00000080824	HSP90AA1	-2.3485	6.01464E-10	8.82744E-08	DN	-1.2700	0.000814049	0.012850047	DN	1.8093
ENSG00000140987	ZSCAN32	-2.0649	1.89849E-09	2.2822E-07	DN	-1.5465	7.95494E-06	0.000274731	DN	1.8057
ENSG00000137203	TFAP2A	-1.7499	6.55682E-06	0.00022155	DN	-1.8045	3.83981E-06	0.000149085	DN	1.7772

DEGs, differentially expressing genes; RNA-seq, RNA sequencing; ID, identification; Sh, short hairpin; DN, DOWN; FC, fold change; adj, adjust; ABS, absolute.

Table 4. Top 10 pathways of KEGG enrichment with accordant DEGs

Pathway	Number of symbols	Proportion of symbols	Symbols	Fold enrichment	*P* value
Notch signaling pathway	16	0.1074	CTBP1, DVL1, NCSTN, KAT2A, DLL1, HDAC1, HES1, NOTCH1, PSENEN, PSEN1, ADAM17, APH1B, MAML2, NUMB, KAT2B, CIR1	15.8233	1.3383E-14
Thyroid hormone signaling pathway	10	0.0671	KAT2A, HDAC1, HRAS, KRAS, MYC, NOTCH1, PLCB4, PLCG2, PRKACB, KAT2B	4.0229	3.4083E-08
PI3K-Akt signaling pathway	20	0.1342	CDK2, COL6A1, PHLPP1, NR4A1, HRAS, HSP90AA1, IGF1, IRS1, ITGA5, ITGB1, KRAS, MYC, NGF, PKN1, RPTOR, BRCA1, THBS1, TLR2, YWHAB, EIF4E2	2.7760	8.1684E-05
Longevity regulating pathway	10	0.0671	CAMKK2, HRAS, IGF1, IRS1, KRAS, PRKACB, RPTOR, CAMKK1, EIF4E2, ULK2	5.0500	0.000130036
Hepatitis B	12	0.0805	CDK2, E2F2, HRAS, KRAS, MYC, NFATC2, CYCS, IFIH1, STAT2, TLR2, YWHAB, CASP10	3.9016	0.000212617
HTLV-I infection	16	0.1074	DVL1, E2F2, KAT2A, HLA-DOA, HRAS, KRAS, MYC, NFATC2, PPP3CB, PRKACB, TBP, WNT2, XBP1, FOSL1, FZD6, KAT2B	2.9439	0.000292248
Wnt signaling pathway	17	0.1141	CTBP1, DVL1, DAAM1, DAAM2, MYC, NFATC2, PLCB4, PPP3CB, PRKACB, PSEN1, SIAH1, WNT2, FOSL1, CAMK2D, FZD6, TCF7L1, NKD2	5.6433	0.000729694
Melanogenesis	9	0.0604	DVL1, HRAS, KRAS, PLCB4, PRKACB, WNT2, CAMK2D, FZD6, TCF7L1	4.2723	0.00104434
Proteoglycans in cancer	13	0.0872	HRAS, IGF1, ITGA5, ITGB1, KRAS, MYC, PLCG2, PRKACB, THBS1, TLR2, WNT2, CAMK2D, FZD6	3.0103	0.001120585
Longevity regulating pathway - multiple species	7	0.0470	HDAC1, HRAS, IGF1, IRS1, KRAS, PRKACB, RPTOR	5.1920	0.001931809

KEGG, Kyoko Encyclopedia of Genes and Genomes; DEGs, differentially expressing genes.

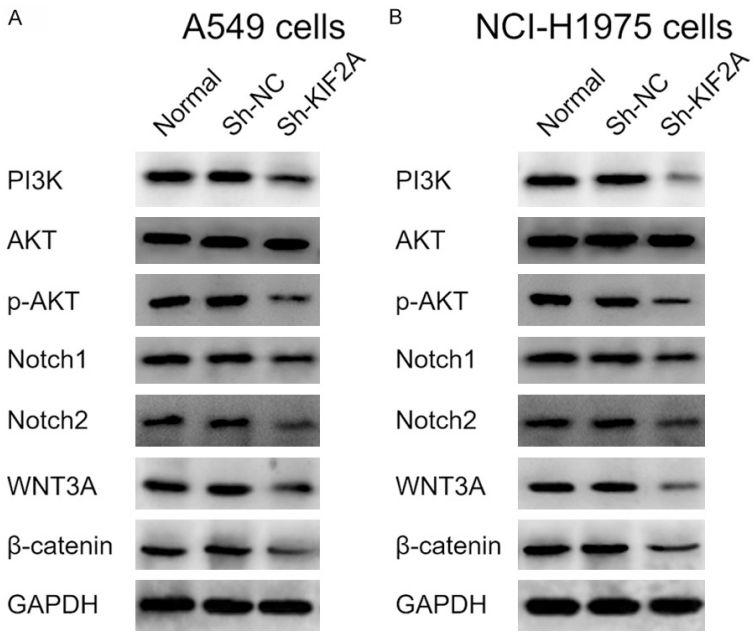

Figure 10. Validation of 3 potential signaling pathway regulated by KIF2A knockdown. Validation of KIF2A knockdown on PI3K-Akt, Wnt and Notch signaling pathways in A549 (A) and NCI-H1975 (B) cells. KIF2A, kinesin family member 2A; Sh, short hairpin RNA; NC, negative control.

inactivating PI3K-Akt signaling pathway in squamous cell carcinoma of oral tongue [21]. Nonetheless, when comes to the molecular mechanism of KIF2A in NSCLC, related evidence is limited, from which we were inspired to explore the molecular mechanism of KIF2A in NSCLC.

Firstly, we detected KIF2A expression in multiple human NSCLC cell lines (A549, NCI-H650, NCI-H358, NCI-H2106, NCI-H1299, NCI-H1650 and NCI-H1975) and human normal lung epithelial cell line (BEAS-2B), then found that KIF2A was upregulated in these NSCLC cell lines compared to BEAS-2B cells. Possible reasons might include the followings: KIF2A might phosphorylate Akt and further activate the oncogenic PI3K-Akt signaling pathway, promoting the initiation and development of NSCLC, therefore, KIF2A was upregulated in NSCLC cell lines compared with normal lung epithelial cell lines. Subsequently, we knocked down KIF2A via ShRNA in A549 and NCI-H1975 cell lines, and then found that KIF2A

knockdown inhibited cell proliferation, invasion in both two cell lines. However, KIF2A knockdown only promoted apoptosis in NCI-H1975 but not in A549 cell line, which might be attributed to the cell-independent phenomenon. Furthermore, KIF2A knockdown decreased N-cadherin expression, but increased E-cadherin expression, suggesting that KIF2A knockdown suppressed EMT progression in NSCLC. We hypothesized that these could be explained by the following probably reasons (1) considering the regulatory effect of KIF2A in mitotic progression, KIF2A knockdown might affect microtubule-dependent mitochondrial fission and alter the duration mitotic progression, further inhibiting cell viability in NSCLC [22]. (2) Given that KIF2A as a depolymerizing motor of microtubule, microtubules dynamics was correlated to activation of EMT progress and tumor cell motility, therefore, we speculated that after KIF2A knockdown, cells might preserve the epithelial features and cease mesenchymal features via a microtubule-dependent manner, which attenuated EMT and cell invasion via stabilizing cytoskeletal microtubules [23]. Following that, we further found that KIF2A knockdown reduced sphere formation ability and $CD133^+$ cells proportion in NSCLC cells, implying that KIF2A knockdown inhibited the stemness of NSCLC cells. The possible reason might involve that, (1) according to previous evidence, EMT progression was correlated with formation as well as the maintenance of cancer cell stemness, KIF2A knockdown might therefore inhibit the self-renewal ability of NSCLC cells via mediating the epithelial and mesenchymal traits of cells in NSCLC [24]. (2) In addition, KIF2A knockdown might inhibit cell stemness traits via inactivating PI3K-Akt and Wnt pathways that regulates stemness in NSCLC, which was further presented in our following RNA-seq data [25].

Current evidence has demonstrated the regulatory effect of KIF2A on chemosensitivity in the treatment of multiple tumors [7, 15, 26]. For instance, depletion of KIF2A synergizes 5-Fluorouracil (5-Fu) on tumor inhibition in squamous cell carcinoma of the oral tongue [26]. Furthermore, another study reports that KIF2A plays a promoting role in the temozolomide-resistance acquirement for glioma cells through PI3K-Akt signaling pathway [14]. In the current study, we conducted further experiments and observed that KIF2A knockdown enhanced the cell chemosensitivity to cisplatin and paclitaxel in NSCLC. In terms of possible reasons that led to these results, they might consist of the followings: (1) based on the current evidence, paclitaxel was a microtubule-stabilizing agent that disrupts malignant cell mitosis, therefore, KIF2A knockdown might synergize with paclitaxel and enhanced the microtubule-stabilizing effect and further reversed the microtubule-directed chemotherapeutic resistance in NSCLC treatment [27]. (2) Furthermore, cisplatin was introduced as an anti-tumor agent via several effective ways (including interfering DNA repair mechanisms, causing DNA damage, mitochondrial malfunction, and further tumor cell apoptosis), hence, KIF2A knockdown might regulate mitochondrial membrane potential and further promote chemosensitivity to cisplatin via mitochondrial fission and fusion machinery [22, 28]. (3) In addition, KIF2A knockdown was speculated to impair cell stemness properties (including tumor initiation, resistance to anti-tumor and immune-targeted therapies, metastatic reactivation and etc.) via inactivating oncogenic gene (such as Notch 2, β-catenin, AKT), and subsequently contributed to the promotion of chemosensitivity of NSCLC cells to cisplatin and paclitaxel [29].

With the purpose of further investigating the molecular mechanism of KIF2A in the pathogenic process of NSCLC, microarray assay and bioinformatic analysis were performed in both A549 and NCI-H1975 cells. It was observed that there were 792 upregulated DEGs and 585 downregulated DEGs by KIF2A knockdown in A549 cells, and 829 upregulated DEGs and 281 downregulated DEGs by KIF2A knockdown in NCI-H1975 cells. Then further cross analysis by Venn diagram illustrated that 292 accordant upregulated DEGs and 64 accordant downregulated DEGs by KIF2A knockdown in both A549 and NCI-H1975 cells. The following KEGG enrichment assay illustrated that these DEGs were mainly enriched in PI3K-Akt, Wnt and Notch signaling pathways. According to the prior evidence, these three signaling pathways serve essential roles in the tumorigenesis of NSCLC, and their activation is correlated with enhanced cell viability and motility, generation of cellular chemoresistance and promoted EMT in NSCLC [30-32]. Considering the aforemen-

tioned evidence, we hypothesized that KIF2A possibly regulated PI3K-Akt, Wnt and Notch signaling pathways in NSCLC, which was further validated by western blotting that KIF2A knockdown decreased protein expressions of PI3K, p-Akt, Notch 1, Notch 2, WNT3A, β-catenin in NSCLC cells. The possible reasons might involve that (1) the KIF2A-mediated DEGs (such as WNT2) might serve as stimulators of PI3K-Akt, Wnt and Notch signaling pathway, hence KIF2A knockdown impaired the activation of these three oncogenic signaling pathways, and further weakened NSCLC progression [31]. (2) According to previous evidence, KIF2A might control the mitochondrial fusion interaction, regulate mitochondrial membrane potential, and alter cell cycling, which subsequently activated pluripotent stem cell identity and established potential stimulating links to cell self-renewal-related PI3K-Akt, Wnt and Notch pathways [22, 25, 33]. Our study provided the evidence for the molecular mechanism of KIF2A in NSCLC, which, however, needed to be validated in further clinical studies.

In conclusion, KIF2A knockdown suppresses NSCLC cell malignant behaviors, EMT and stemness, but enhances chemosensitivity via inactivating PI3K-Akt, Wnt, and Notch signaling pathways, which enriches the understanding of NSCLC pathological progress as well as proposes a potential therapeutic target for NSCLC treatment.

Disclosure of conflicts of interest

None.

Address correspondence to: Zhen Zhang and Min Fan, Department of Radiation Oncology, Fudan University Shanghai Cancer Center, Shanghai, China; Department of Oncology, Shanghai Medical College, Fudan University, Shanghai, China. Tel: +86-021-64175590; E-mail: zhenzhang6@gmail.com (ZZ); fanming@fudan.edu.cn (MF)

References

[1] Osmani L, Askin F, Gabrielson E and Li QK. Current WHO guidelines and the critical role of immunohistochemical markers in the subclassification of non-small cell lung carcinoma (NSCLC): moving from targeted therapy to immunotherapy. Semin Cancer Biol 2018; 52: 103-109.

[2] Nagasaka M and Gadgeel SM. Role of chemotherapy and targeted therapy in early-stage non-small cell lung cancer. Expert Rev Anticancer Ther 2018; 18: 63-70.

[3] Arbour KC and Riely GJ. Systemic therapy for locally advanced and metastatic non-small cell lung cancer: a review. JAMA 2019; 322: 764-774.

[4] Valentino F, Borra G, Allione P and Rossi L. Emerging targets in advanced non-small-cell lung cancer. Future Oncol 2018; 14: 61-72.

[5] Ettinger DS, Aisner DL, Wood DE, Akerley W, Bauman J, Chang JY, Chirieac LR, D'Amico TA, Dilling TJ, Dobelbower M, Govindan R, Gubens MA, Hennon M, Horn L, Lackner RP, Lanuti M, Leal TA, Lilenbaum R, Lin J, Loo BW, Martins R, Otterson GA, Patel SP, Reckamp K, Riely GJ, Schild SE, Shapiro TA, Stevenson J, Swanson SJ, Tauer K, Yang SC, Gregory K and Hughes M. NCCN guidelines insights: non-small cell lung cancer, version 5.2018. J Natl Compr Canc Netw 2018; 16: 807-821.

[6] Walczak CE, Gayek S and Ohi R. Microtubule-depolymerizing kinesins. Annu Rev Cell Dev Biol 2013; 29: 417-441.

[7] Li X, Shu K, Wang Z and Ding D. Prognostic significance of KIF2A and KIF20A expression in human cancer: a systematic review and meta-analysis. Medicine (Baltimore) 2019; 98: e18040.

[8] Yi ZY, Ma XS, Liang QX, Zhang T, Xu ZY, Meng TG, Ouyang YC, Hou Y, Schatten H, Sun QY and Quan S. Kif2a regulates spindle organization and cell cycle progression in meiotic oocytes. Sci Rep 2016; 6: 38574.

[9] Gilbert SP, Guzik-Lendrum S and Rayment I. Kinesin-2 motors: kinetics and biophysics. J Biol Chem 2018; 293: 4510-4518.

[10] Zhang X, Wang Y, Liu X, Zhao A, Yang Z, Kong F, Sun L, Yu Y and Jiang L. KIF2A promotes the progression via AKT signaling pathway and is upregulated by transcription factor ETV4 in human gastric cancer. Biomed Pharmacother 2020; 125: 109840.

[11] Xie T, Li X, Ye F, Lu C, Huang H, Wang F, Cao X and Zhong C. High KIF2A expression promotes proliferation, migration and predicts poor prognosis in lung adenocarcinoma. Biochem Biophys Res Commun 2018; 497: 65-72.

[12] Wang G, Wang Z and Yu H. Kinesin family member 2A high expression correlates with advanced tumor stages and worse prognosis in non-small cell lung cancer patients. J Clin Lab Anal 2020; 34: e23135.

[13] Zhao P, Lan F, Zhang H, Zeng G and Liu D. Down-regulation of KIF2A inhibits gastric cancer cell invasion via suppressing MT1-MMP. Clin Exp Pharmacol Physiol 2018; 45: 1010-1018.

[14] Yin H and Cui X. Knockdown of circHIPK3 facilitates temozolomide sensitivity in glioma by regulating cellular behaviors through miR-524-5p/KIF2A-mediated PI3K/AKT pathway. Cancer Biother Radiopharm 2020; [Epub ahead of print].
[15] Schimizzi GV, Currie JD and Rogers SL. Expression levels of a kinesin-13 microtubule depolymerase modulates the effectiveness of anti-microtubule agents. PLoS One 2010; 5: e11381.
[16] Head SR, Komori HK, LaMere SA, Whisenant T, Van Nieuwerburgh F, Salomon DR and Ordoukhanian P. Library construction for next-generation sequencing: overviews and challenges. Biotechniques 2014; 56: 61-64, 66, 68, passim.
[17] Huang DW, Sherman BT, Tan Q, Kir J, Liu D, Bryant D, Guo Y, Stephens R, Baseler MW, Lane HC and Lempicki RA. DAVID bioinformatics resources: expanded annotation database and novel algorithms to better extract biology from large gene lists. Nucleic Acids Res 2007; 35: W169-175.
[18] Seira O, Liu J, Assinck P, Ramer M and Tetzlaff W. KIF2A characterization after spinal cord injury. Cell Mol Life Sci 2019; 76: 4355-4368.
[19] Parrini E, Conti V, Dobyns WB and Guerrini R. Genetic basis of brain malformations. Mol Syndromol 2016; 7: 220-233.
[20] Ogawa T and Hirokawa N. Microtubule destabilizer KIF2A undergoes distinct site-specific phosphorylation cascades that differentially affect neuronal morphogenesis. Cell Rep 2015; 12: 1774-1788.
[21] Wang K, Lin C, Wang C, Shao Q, Gao W, Song B, Wang L, Song X, Qu X and Wei F. Silencing Kif2a induces apoptosis in squamous cell carcinoma of the oral tongue through inhibition of the PI3K/Akt signaling pathway. Mol Med Rep 2014; 9: 273-278.
[22] Horbay R and Bilyy R. Mitochondrial dynamics during cell cycling. Apoptosis 2016; 21: 1327-1335.
[23] Pongrakhananon V, Wattanathamsan O, Takeichi M, Chetprayoon P and Chanvorachote P. Loss of CAMSAP3 promotes EMT via the modification of microtubule-Akt machinery. J Cell Sci 2018; 131: jcs216168.
[24] Pradella D, Naro C, Sette C and Ghigna C. EMT and stemness: flexible processes tuned by alternative splicing in development and cancer progression. Mol Cancer 2017; 16: 8.
[25] Rasmussen ML, Ortolano NA, Romero-Morales AI and Gama V. Wnt signaling and its impact on mitochondrial and cell cycle dynamics in pluripotent stem cells. Genes (Basel) 2018; 9: 109.
[26] Wang CQ, Li YJ, Wei ZM, Zhu CJ, Qu X, Wei FC, Xing XM and Yu WJ. Stable gene-silence of Kif2a synergistic with 5-fluorouracil suppresses oral tongue squamous cell carcinoma growth in vitro and in vivo. Oral Surg Oral Med Oral Pathol Oral Radiol 2013; 116: 49-54.
[27] Weaver BA. How Taxol/paclitaxel kills cancer cells. Mol Biol Cell 2014; 25: 2677-2681.
[28] Dasari S and Tchounwou PB. Cisplatin in cancer therapy: molecular mechanisms of action. Eur J Pharmacol 2014; 740: 364-378.
[29] Wang X, Meng Q, Qiao W, Ma R, Ju W, Hu J, Lu H, Cui J, Jin Z, Zhao Y and Wang Y. miR-181b/Notch2 overcome chemoresistance by regulating cancer stem cell-like properties in NSCLC. Stem Cell Res Ther 2018; 9: 327.
[30] Ram Makena M, Gatla H, Verlekar D, Sukhavasi S, K Pandey M and C Pramanik K. Wnt/beta-catenin signaling: the culprit in pancreatic carcinogenesis and therapeutic resistance. Int J Mol Sci 2019; 20: 4242.
[31] Zou B, Zhou XL, Lai SQ and Liu JC. Notch signaling and non-small cell lung cancer. Oncol Lett 2018; 15: 3415-3421.
[32] Perez-Ramirez C, Canadas-Garre M, Molina MA, Faus-Dader MJ and Calleja-Hernandez MA. PTEN and PI3K/AKT in non-small-cell lung cancer. Pharmacogenomics 2015; 16: 1843-1862.
[33] Katoh M. Canonical and non-canonical WNT signaling in cancer stem cells and their niches: cellular heterogeneity, omics reprogramming, targeted therapy and tumor plasticity (Review). Int J Oncol 2017; 51: 1357-1369.